Electronic Supplementary Information

BaB$_8$O$_{12}$F$_2$: A Promising Deep-UV Birefringent Material

Zhizhong Zhang,[#ab] Ying Wang,[#a] Hao Li,[ab] Zhihua Yang[a] and Shilie Pan*[ab]

[a]CAS Key Laboratory of Functional Materials and Devices for Special Environments, Xinjiang Technical Institute of Physics & Chemistry, CAS; Xinjiang Key Laboratory of Electronic Information Materials and Devices, 40-1 South Beijing Road, Urumqi 830011, China.
[b]Center of Materials Science and Optoelectronics Engineering，University of Chinese Academy of Sciences, Beijing 100049, China

Experimental Section

Synthesis

Polycrystalline samples synthesis of $BaB_8O_{12}F_2$ was performed by the traditional solid-state reaction in closed systems. The starting material $Ba(BF_4)_2$ was synthesized by the reaction of $BaCO_3$ (Tianjin Yao Hua Chemical Reagent Co., Ltd., 99.0%) and excess amount of HBF_4 (Aladdin AR, 40 wt%). After filtration, the obtained colorless powder was further dried in vacuum at 120 °C. Then, a mixture of as-synthesized $Ba(BF_4)_2$ and H_3BO_3 (Tianjin Baishi Chemical Reagent Co., Ltd., 99.5%) with a molar ratio of 1 : 8 was placed in a corundum crucible, then burned in muffle furnace from 200 to 300 °C with several intermediate grinding. Then the precursors (0.5 g) were moved into a fused-silica tube and flame-sealed under a high vacuum of 10^{-3} Pa. The tubes were then placed into a computer-controlled furnace, heated to 400 °C during 7 h, held at 400 °C for 150 h, and finally cooled to room temperature at a rate of 2 °C/h. The polycrystalline powder of $BaB_8O_{12}F_2$ was obtained. The phase purity was confirmed by powder X-ray diffraction, which was carried on a Bruker D2 PHASER diffractometer with Cu $K\alpha$ radiation at room temperature.

Single crystals of $BaB_8O_{12}F_2$ were grown by high-temperature flux method in a closed system. A mixture of BaF_2 (0.088 g, 0.5 mmol), B_2O_3 (0.278 g, 2 mmol) and KBF_4 (0.126 g 1 mmol) were loaded into a 10 mm (inner diameter) fused-silica tube. The silica tube was sealed with methane-oxygen flame under a high vacuum of 10^{-3} Pa. Then, the tube was placed in a computer-controlled furnace, heated to 550 °C in 12 h, dwelled at 550 °C for 20 h, cooled to 50 °C at a rate of 2 °C/h, and finally cooled to room temperature by switching off the furnace. After that, colorless $BaB_8O_{12}F_2$ single crystals were obtained.

Characterization.

Single crystal diffraction data were collected on a Bruker SMART APEX II CCD diffractometer using monochromatic Mo $K\alpha$ radiation at room temperature. The initial crystal structures were solved by direct methods and then refined with anisotropic displacement parameters for all atoms using the SHELXTL program package.[1] The structures were verified by PLATON and no higher symmetry elements were found.[2] Crystal data and structure refinement information are given in Table S1. The final refined atomic positions, isotropic thermal parameters and bond valence sum (BVS) calculations of the atoms are summarized in Table S2. Selected bond distances (Å) and angles (deg) are listed in Table S3.

Elemental analysis was carried on the clean single crystal surface with the aid of a SUPRA 55VP field emission scanning electron microscope equipped with a Bruker x-flash-sdd-5010 energy dispersive X-ray (EDX) spectroscope. Infrared spectroscopy was carried out on a Shimadzu IR Affinity-1 Fourier transform infrared spectrometer in the 400–4000 cm^{-1} range. Thermal gravimetric analysis (TGA) and differential scanning calorimetry (DSC) were carried out on a simultaneous NETZSCH STA 449 F3 thermal analyzer instrument in a flowing N_2 atmosphere. Polycrystalline $BaB_8O_{12}F_2$ was placed in a Pt crucible, heated from 40 to 1000 °C at a rate of 10 °C min^{-1}. Ultraviolet–visible–near infrared diffuse-reflectance spectroscopy data in the wavelength range of 180–1600 nm was recorded at room temperature using a powder

sample of $BaB_8O_{12}F_2$ on a Shimadzu SolidSpec-3700 DUV spectrophotometer.

Computational methods.

The first-principles calculations were performed by the plane-wave pseudopotential method implemented in the CASTEP software package.[3] The exchange-correlation potential was calculated using Perdew-Burke-Ernzerhof (PBE) functional within the generalized gradient approximation (GGA).[4] To achieve energy convergence, the kinetic energy cutoff of 940 eV for $BaB_8O_{12}F_2$, 830 eV for α-BaB_2O_4 within normal-conserving pseudopotential (NCP) was adopted.[5-6] The Monkhorst–Pack k-point meshes in the Brillouin zone were set as $4 \times 4 \times 4$ for $BaB_8O_{12}F_2$ and α-BaB_2O_4. For calculations, we adopted geometry optimization, *i.e.*, the cell parameters and the atomic coordinates of all the atoms were optimized. The geometry optimization was converged when the residual forces on the atoms were less than 0.01 eV/Å, the displacements of atoms were less than 5×10^{-4} Å, and the energy change was less than 5.0×10^{-6} eV/atom. On the basis of the band structure, the linear optical refractive indices and birefringence can be obtained by the real part of dielectric function.

Table S1 Crystal data and structure refinement for $BaB_8O_{12}F_2$.

Empirical formula	$BaB_8O_{12}F_2$
Formula weight	453.82
Temperature	296(2) K
Wavelength	0.71073 Å
Crystal system	Trigonal
Space group	$R\bar{3}c$
Unit cell dimensions	$a = 6.6824(4)$ Å
	$c = 35.964(5)$ Å
Volume	1390.8(2) Å^3
Z	6
Density (calculated)	3.251 mg/m^3
Absorption coefficient	4.399 mm^{-1}
F(000)	1260
Crystal size	$0.22 \times 0.13 \times 0.11$ mm^3
Theta range for data collection	3.40 to 27.54°.
Index ranges	$-7 \leq h \leq 8, -8 \leq k \leq 8, -46 \leq l \leq 43$
Reflections collected	2546
Independent reflections	365 [R(int) = 0.0249]
Completeness to theta = 27.54°	100.00%
Refinement method	Full-matrix least-squares on F^2
Data / restraints / parameters	365 / 0 / 36
Goodness-of-fit on F^2	1.130
Final R indices [$I > 2sigma(I)$][a]	$R_1 = 0.0150, wR_2 = 0.0427$
R indices (all data)[a]	$R_1 = 0.0189, wR_2 = 0.0457$
Largest diff. peak and hole	0.414 and -0.414 e/Å^3

[a] $R_1 = \Sigma||F_o| - |F_c||/\Sigma|F_o|$ and $wR_2 = [\Sigma w(F_o^2 - F_c^2)^2 / \Sigma w\, F_o^4]^{1/2}$ for $F_o^2 > 2\sigma(F_o^2)$

Table S2 Atomic coordinates ($\times 10^4$), equivalent isotropic displacement parameters ($\text{Å}^2 \times 10^3$) and BVS of each atom for $BaB_8O_{12}F_2$. U(eq) is defined as one third of the trace of the orthogonalized U_{ij} tensor.

Atom	x	y	z	U(eq)	BVS
Ba(1)	6667	3333	833	10(1)	2.186
B(1)	6667	3333	-338(1)	7(1)	3.096
B(2)	722(5)	2357(5)	434(1)	9(1)	3.011
O(1)	2322(3)	1615(3)	423(1)	10(1)	1.923
O(2)	3283(3)	-1282(3)	470(1)	10(1)	2.000
F(1)	6667	3333	51(1)	16(1)	0.966

Table S3 Selected bond lengths [Å] and angles [deg] for $BaB_8O_{12}F_2$.

Ba(1)-O(1)[#1]	2.9307(19)	B(1)-O(2)[#8]	1.467(2)
Ba(1)-O(1)[#2]	2.9308(19)	B(1)-F(1)	1.402(6)
Ba(1)-O(1)[#3]	2.9307(19)	B(2)-O(1)	1.386(3)
Ba(1)-O(1)[#4]	2.9307(19)	B(2)-O(1)[#9]	1.391(3)
Ba(1)-O(1)	2.9307(19)	B(2)-O(2)[#9]	1.335(4)
Ba(1)-O(1)[#5]	2.9307(19)	O(2)[#6]-B(1)-O(2)[#8]	110.03(19)
Ba(1)-O(2)[#1]	3.0587(18)	O(2)[#6]-B(1)-O(2)[#7]	110.03(19)
Ba(1)-O(2)[#5]	3.0587(18)	O(2)[#8]-B(1)-O(2)[#7]	110.03(19)
Ba(1)-O(2)[#2]	3.0587(18)	F(1)-B(1)-O(2)[#6]	108.9(2)
Ba(1)-O(2)	3.0587(18)	F(1)-B(1)-O(2)[#7]	108.9(2)
Ba(1)-F(1)[#4]	2.812(3)	F(1)-B(1)-O(2)[#8]	108.9(2)
Ba(1)-F(1)	2.812(3)	O(1)-B(2)-O(1)[#9]	118.5(2)
B(1)-O(2)[#6]	1.467(2)	O(2)[#9]-B(2)-O(1)[#9]	117.6(2)
B(1)-O(2)[#7]	1.467(2)	O(2)[#9]-B(2)-O(1)	123.9(2)

Symmetry transformations used to generate equivalent atoms:

#1 -y+1, x-y, z   #2 -x+y+1, -x+1, z   #3 x-y+1/3, -y+2/3, -z+1/6
#4 y+1/3, x-1/3, -z+1/6   #5 -x+4/3, -x+y+2/3, -z+1/6
#6 -x+1, -y, -z   #7 x-y, x, -z   #8 y+1, -x+y+1, -z
#9 -y, x-y, z   #10 x-1, y, z   #11 -x+y, -x, z

Figure S1. PXRD patterns of $BaB_8O_{12}F_2$.
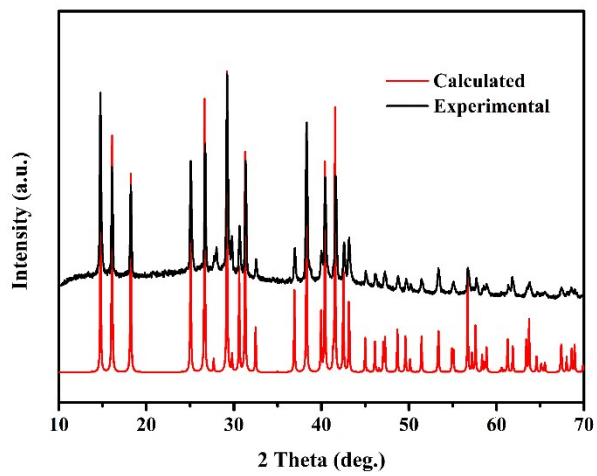
Figure S2. Elemental analysis. Energy dispersive X-ray spectroscopy (EDX) was performed to verify the absence or presence of the F and O atoms because the X-ray diffraction cannot distinguish the two atoms. The EDX analysis indicates that the molar ratio of Ba:B:O:F is 1:7.88:12.13:1.96, which is approximately equal to the theoretical molar ratio of 1:8:12:2. The result further verifies that fluorine indeed exists in the crystal structure.
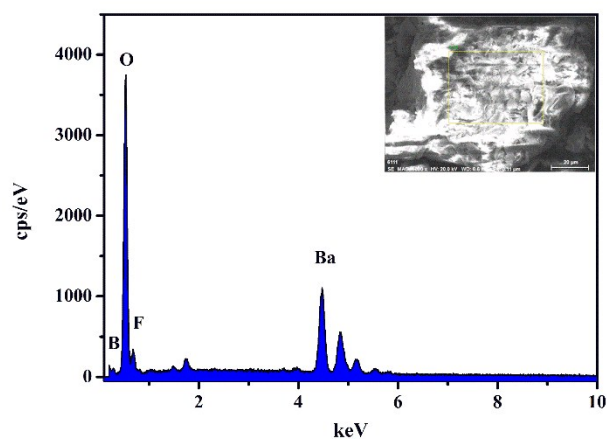
Figure S3. A and A′ $[B_4O_6F]_\infty$ layers in opposite direction (a) along the a axis, (b) along the c axis.
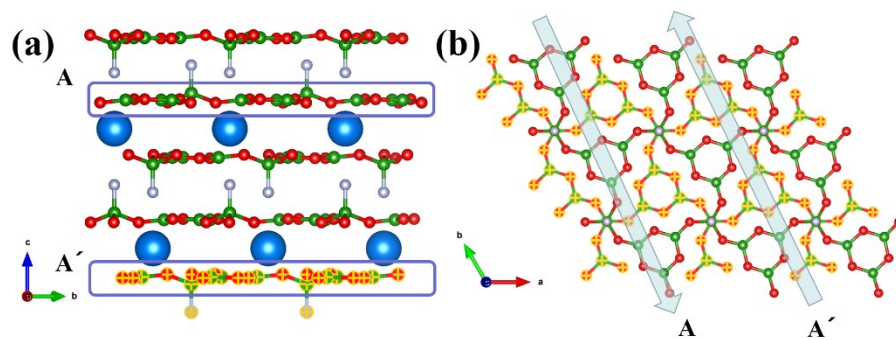
Figure S4. Thermal behavior of $BaB_8O_{12}F_2$.

(a)

(b)
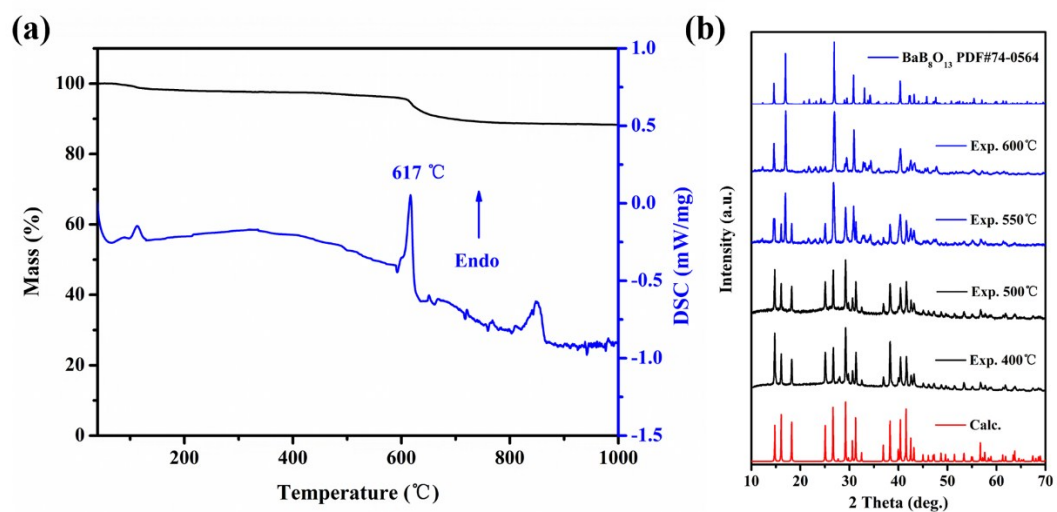
Figure S5. IR spectrum of $BaB_8O_{12}F_2$. According to the references,[7-9] the following absorption peaks are assigned. The peak near 860 cm^{-1} comes from the B−O symmetric stretching of BO_3. The out-of-plane bending mode of BO_3 generates two absorption peaks around 712 and 598 cm^{-1}. The peak close to 500 cm^{-1} characterizes bending modes of BO_3. The absorption peaks in the range of 1420-1370 cm^{-1} are attributed to the B−O asymmetric stretching vibration of BO_3. This result indicates that the coordination environment of the BO_3 triangles of $BaB_8O_{12}F_2$ is analogue to that of CsB_4O_6F, that is, three BO_3 triangles form a B_3O_6 ring. The peak near 1047 and 862 cm^{-1} originates from the B−F asymmetric and symmetric stretching vibration of BO_3F tetrahedra, respectively. The results verify the presence of the B_3O_6 and BO_3F tetrahedra, which is consistent with the structural analysis.
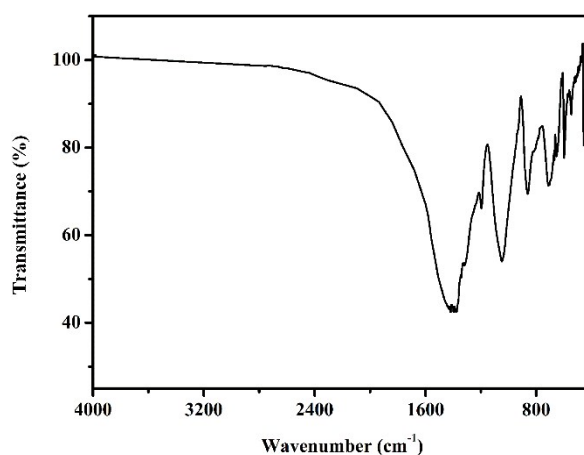
Figure S6. The projected density of states of (a) $BaB_8O_{12}F_2$ and (b) α-BaB_2O_4.
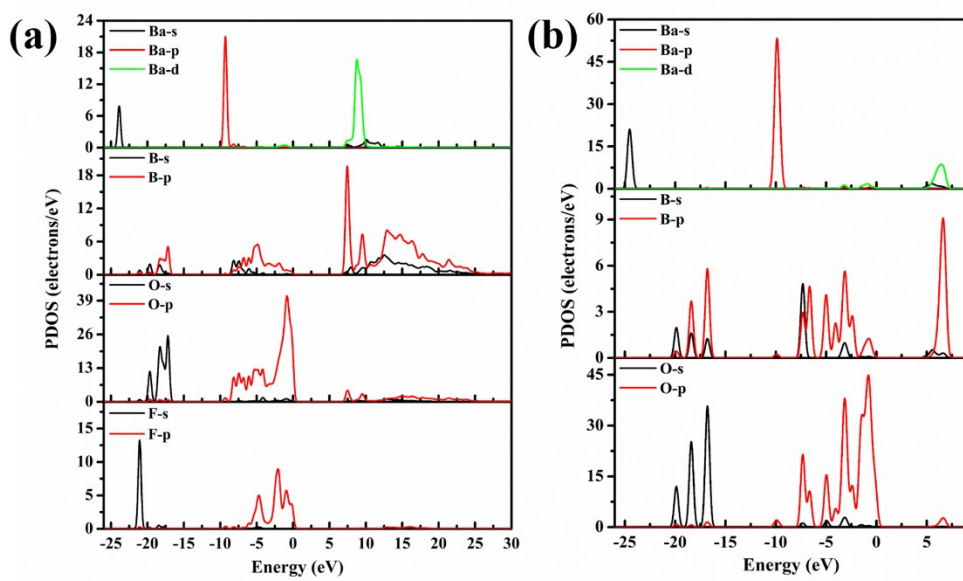
References

1   G. M. Sheldrick, *Acta Crystallogr. A*, 2015, **71**, 3.

2   A. L. J. Spek, *J. Appl Crystallogr.*, 2003, **36**, 7.

3   S. J. Clark, M. D. Segall, C. J. Pickard, P. J. Hasnip, M. I. Probert, K. Refson and M. C. Payne, *Z. Kristallogr. Cryst. Mater.*, 2005, **220**, 567.

4   J. P. Perdew, K. Burke and M. Ernzerhof, *Phys. Rev. Lett.*, 1996, **77**, 3865.

5   J. S. Lin, A. Qteish, M. C. Payne and V. Heine, *Phys. Rev. B*, 1993, **47**, 4174.

6   A. M. Rappe, K. M. Rabe, E. Kaxiras and J. D. Joannopoulos, *Phys. Rev. B*, 1990, **41**, 1227.

7   G. P. Han, Y. Wang, B. B. Zhang and S. L. Pan, *Chem.–Eur. J.*, 2018, **24**,17638.

8   S. J. Han, Y. Wang, B. B. Zhang, Z. H. Yang and S. L. Pan, *Inorg. Chem.*, 2018, **57**, 873.

9   S. G. Jantz, F. Pielnhofer, L. van Wüllen, R. Weihrich, M. J. Schäfer and H. A. Höppe, *Chem.–Eur. J.*, 2018, **24**, 443.